

IPMU-11-0121

UT-11-23

KEK-TH-1478

LHC Test of CDF Wjj anomaly

Keisuke Harigaya^{1,2}, Ryosuke Sato^{1,2}, and Satoshi Shirai³

¹*Institute for the Physics and Mathematics of the Universe, University of Tokyo,
Kashiwa 277-8568, Japan*

²*Department of Physics, University of Tokyo,
Tokyo 113-0033, Japan*

³*Institute of Particle and Nuclear Studies,
High Energy Accelerator Research Organization (KEK)
Tsukuba 305-0801, Japan*

Abstract

We discuss a test of the CDF dijet anomaly at the LHC. The recent observed dijet mass peak at the CDF is well fitted by a new particle with a mass of around 150 GeV, which decays into two jets. In this paper, we focus on only Wjj signal to avoid model dependence, and comprehensively study the LHC discovery/exclusion reach. We found almost all the models are inconsistent with the result of the LHC, unless only valence quarks contribute the new process. We also discuss further prospects of the LHC search for this anomaly.

1 Introduction

Recently, the CDF collaboration reported an anomaly in Wjj events [1]. This result indicates a new particle X with mass around 150 GeV and the production cross section associated with a W boson is around 4 pb at the Tevatron. There are many models proposed to explain this anomaly [2, 3, 4, 5, 6]. Since the D0 collaboration reports result inconsistent with the CDF [7], it is very important to test the Wjj anomaly at the LHC.

Each model can have individual manner to be tested. Some model may predict the collider signals other than Wjj . For example, Ref. [8] discusses the testing at the LHC for the Technicolor model by using various modes. However, the discussion using modes other than Wjj is strongly model dependent. In this paper, we focus on only Wjj signal at the LHC to test various models with model independent manner, regardless of such other considerations. We discuss possible effective interactions and resonant particles which give the Wjj signal. Then, our study does not depend on the detail of the model and we can cover almost all the model in other references. When we discuss the various models, we do not care about the flavor symmetry violation or the deviation from the electroweak precision test. To discuss them, we have to specify the whole of the model. Furthermore, some other particles unrelated to Wjj signal may compensate such a violation, then, the comprehensive study is difficult. We study models which can realize Wjj signal at the Tevatron, and discussed the expected signal cross section at the LHC. We found that almost all models can be discovered or excluded at the LHC.

2 Setup

A lot of models proposed to explain the CDF dijet anomaly assume tree level s-channel or t-channel process¹ whose final state is a W boson and a new particle X with a mass of around 150 GeV. In this paper, we consider the following two cases:

Case 1: W boson and X are produced without WX invariant mass peak.

In this case, to test the models with model independent manners, we concentrate

¹ There are some models which can not be classified to such a class. For example, in some models [4], new particles are pair-produced at first, and a W boson and jj are generated from each new particle decay.

on the effective theory. We consider the cases in which the particle X is described by scalar, spinor and vector field. We have considered possible effective operators to provide a process $p\bar{p} \rightarrow WX$ up to dimension 5. In constructing the effective operators, we have respected the $SU(3)_C \times SU(2)_L \times U(1)_Y$ gauge symmetry and the Lorentz symmetry but allowed the operators which can arise by the standard model higgs condensation.

Case 2: another particle Y is produced by s-channel then it decays into a W boson and X .

A resonant behavior of Wjj signal is constrained from $m_{\ell\nu jj}$ distribution, but $m_{\ell\nu jj}$ peak around 280 GeV is less constrained [9]. So, we can consider another particle Y with the mass of 280 GeV, and WX signal is generated by the following process:

$$p + \bar{p} \rightarrow Y \rightarrow W + X.$$

We have concentrated on the case in which the narrow width approximation is valid. In this way, we can give a model-independent result.

We also assumed that the CP invariance is preserved at the level of effective operators. That is, when an effective operator is introduced, its hermite conjugate operator is also introduced.

3 Constrains from hadron collider experiments

3.1 LHC

Here, we discuss the discovery/exclusion reach at the LHC 7 TeV run. The ATLAS group shows dijet invariant mass M_{jj} distribution associated with a W boson with 1.02 fb^{-1} data [10]. This data is consistent with the standard model background, then, it gives a severe constraint on the WX cross section at the LHC. The ATLAS groups shows the data with third jet veto and the data without veto. The data without veto gives more severe constraint on the cross section, because third jet veto significantly decreases signal acceptance while the background can not be so reduced. In the following of this section, we use the data without third jet veto.

Table 1: The current and expected upper bounds of WX cross section at 95% C.L. in the LHC 7 TeV run. The row shows each integrated luminosity. The most bottom row shows the limit when statistical error can be neglect. The column shows the size of systematic error. In the left column we take the same systematic error as Ref. [10], In the middle column we take the half of the systematic error as Ref. [10], In the right column we take only statistical error.

	sys.err. = Ref. [10]	sys.err. = $\frac{1}{2}$ Ref. [10]	only stat.err.
1.02 fb^{-1}	16.7 pb	12.9 pb	11.1 pb
$1.02 \text{ fb}^{-1} \times 2$	15.9 pb	11.6 pb	9.3 pb
$1.02 \text{ fb}^{-1} \times 4$	15.4 pb	10.8 pb	7.9 pb
$1.02 \text{ fb}^{-1} \times \infty$	15.0 pb	10.0 pb	

When the decay width of X is small enough compared to the jet resolution, WX events may give significant contribution to M_{jj} distribution around 150 GeV. We estimate signal acceptance for the event cut used in Ref. [10] by using MadGraph-Pythia-PGS package [11]. Given signal acceptance, we can estimate the upper bound of WX cross section by simple event number counting. We estimate the upper bound of WX cross section at 95% C.L. by using the RooStats tools [12]. We can get the upper bound as 16.7 pb from the present ATLAS data.²

In the following of this paper, we discuss the LHC discovery/exclusion by using enhancement factor R_{LHC} , which is defined by the ratio of cross section between at the LHC 7 TeV run and at the Tevatron, such as,

$$R_{\text{LHC}} = \frac{\sigma(pp \rightarrow WX; \sqrt{s} = 7 \text{ TeV})}{\sigma(p\bar{p} \rightarrow WX; \sqrt{s} = 1.96 \text{ TeV})}. \quad (1)$$

By using the upper bound of the cross section, we can get the upperbound of R_{LHC} . To estimate this bound conservatively, we take the cross section 2 pb at the Tevatron in Eq. (1). Then, R_{LHC} have to be lower than 8.4. This value gives stringent constraint on the model which gives Wjj signal. The more integrated luminosity and the less systematic error can give more severe upper bound. The result is given by Table 1.

² We fixed signal acceptance when we estimate the bound of the cross section. In fact, signal acceptance slightly depends on the particle property and its interaction. Roughly, its dependence is a few ten percent, which can be ignored in our conservative estimation of the upper bound on R_{LHC} .

3.2 Sp̄pS

Some model predicts the single production of X by the quark or gluon fusion at hadron colliders. Due to the low energy kinematical cut, low energy hadron collider can set good constraints on the production cross section of X decaying into dijet. We utilized the results of the UA2 collaboration [13], which give the constraints on the production cross section times the branching ratio to dijet of excited vector boson and quark. There are two things to be noticed.

First, the sensitivity of dijet search depends on the decay width of the parent particle, because a broad width weakens the constraint from the dijet search. The UA2 analysis assumed the particular value for the decay width of the produced particle. However, the assumed width is smaller than the mass resolution, which is about 10 % of the mass of the parent particle. Therefore, we can apply their constraints on the production cross section if the decay width is smaller than $150 \times 0.1 = 15$ GeV. To be conservative, we do not apply the UA2 constraint to the particle whose decay width is larger than 15 GeV.

Second, the sensitivity also depends on the decay mode of the parent particle. A heavy quark jet (i.e, c and b quark) loses its energy due to the decay of the heavy quark. This results in the existence of low energy tail in the dijet mass distribution, which lowers the sensitivity of dijet peak search. Therefore, the upperbound of the cross section becomes loose if X decays into a heavy quark. However, as we will see in the following of this paper, X coupling to a heavy quark is severely constrained at the LHC. Therefore, if we concentrate on a model which does not excluded by the LHC, we can adopt the constraint for the particle only decay into light quarks or gluon. The upper limit for the production cross section of X is 80 pb at 90 % C.L. In the same way as the constraint from the ATLAS result, we discuss the exclusion/discovery by using the ratio of the cross section at the Sp̄pS and the Tevatron. We defined the ratio of cross section, such as,

$$R_{\text{Sp̄pS}} = \frac{\sigma(p\bar{p} \rightarrow X; \sqrt{s} = 540 \text{ GeV})}{\sigma(p\bar{p} \rightarrow WX; \sqrt{s} = 1.96 \text{ TeV})}. \quad (2)$$

To estimate the upperbound of $R_{\text{Sp̄pS}}$ conservatively, we take the cross section at the Tevatron to be 2 pb in Eq. (2). Then, $R_{\text{Sp̄pS}}$ have to be lower than 40.

4 Non-resonant production

We classify the effective operators by X 's spin and its coupling to the standard model particles. Note that in the case W boson's interaction is same as that of the standard model, X must couple to the left-handed quarks. We summarize the operators we considered in Table 2. We assume that only one operator mainly contributes to the production of X and W boson at the Tevatron. As for the operators not listed there, we give some comments in the following subsections. If we require the cross section of WX signal to be 4 pb at the Tevatron, we can get the required coupling constant. However, the coupling constant depends on the normalization, for example, definition of tensor which suppress $SU(3)_C \times SU(2)_L \times U(1)_Y$ indexes. Therefore, in this section, we discuss the required decay width instead of the coupling constant. We discuss physical quantity, then, we can avoid the confusion of the normalization.

Note that some operators do not make X decay into dijet, i.e., $G_{\mu\nu}W^{\mu\nu}\phi$, $B_{\mu\nu}W^{\mu\nu}\phi$, $G_{\mu\nu}W^\mu V^\nu$ and $W_{\mu\nu}^3 W^\mu V^\nu$ in Table 2. In these cases, in addition to the original interaction, we must add another interaction which forces X to decay into dijet. To avoid the suppression of the cross section by branching ratio, we have to assume the decay interaction as strong as the original interaction. This makes the analysis complicated, because the decay interaction also contributes to the production process. However, the original interaction always produces X and W boson by the SM gauge boson s-channel process. Then, the production cross section is dominated by the process with the initial parton to be valence quark. In order to dominate the production cross section of WX signal for the original operator, we have to assume the decay interaction forces X to decay into sea quarks. For the sea quark the factor R_{LHC} is larger than valence quark, the operator introduced to makes X decay enhances R_{LHC} . Therefore, adding the interaction which forces X decay into dijet improve the exclusion with the LHC. Therefore, in the case the LHC can exclude the operator we are considering without adding another operator which contributes to the decay into dijet, we do not further analyze with another operator.

In this section and the next section, we estimate a cross section at the hadron colliders by convoluting a parton level cross section with parton distribution functions. We have used CTEQ 6.1 PDF [14].

Table 2: List of the operators we considered. ϕ , V , ψ_L is the new particle with spin 0, 1, 1/2 respectively. Options for $U(1)_Y$ charges are determined by whether q_R is up-type or down-type quark.

Interaction	$SU(3)_C$	$SU(2)_L$	$U(1)_Y$	Section
$\phi q_L^\dagger q_R$	1 or 8	2	$\pm 1/2$	4.1.1
$\phi q_L^\dagger q_R^c$	$\bar{3}$ or 6	1 or 3	1/3	4.1.1
$G_{\mu\nu}^a W^{\mu\nu} \phi^a$	8	3	0	4.1.2
$B_{\mu\nu} W^{\mu\nu} \phi$	1	3	0	4.1.3
$V^\mu q_L^\dagger \bar{\sigma}_\mu q_L$,	1 or 8	1 or 3	0	4.2.1
$V^\mu q_L^\dagger \bar{\sigma}_\mu q_L^c$	$\bar{3}$ or 6	2	5/6 or -1/6	4.2.1
$V_{\mu\nu} q_L^{c\dagger} \sigma^{\mu\nu} q_L$	3 or $\bar{6}$	1 or 3	-1/3	4.2.2
$V_{\mu\nu} q_R^\dagger \sigma^{\mu\nu} q_L$	1 or 8	2	$\pm 1/2$	4.2.2
$G_{\mu\nu}^a W^\mu V^{a\nu}$ (arise from $G_{\mu\nu}^a D^\mu V^{a\nu} H$)	8	2	1/2	4.2.3
$W_{\mu\nu}^3 W^\mu V^\nu$ (arise from $W_{\mu\nu}^i (D^\mu V^\nu)^i$)	1	3	0	4.2.4
$G_{\mu\nu} q_L^{c\dagger} \sigma^{\mu\nu} \psi_L$	$\bar{3}$ or 6 or 15	2	-1/6	4.3.1

4.1 $X = \phi$: scalar particle

4.1.1 Quark- Quark- ϕ

The possible operators are

$$\phi q_L^\dagger q_R \text{ or } \phi q_L^\dagger q_R^c. \quad (3)$$

and their conjugates. These interaction terms give $W\phi$ signal by t-channel quark exchange diagrams. The cross section of Wjj signal is proportional to $N_\phi \Gamma(\phi \rightarrow qq)$, where $\Gamma(\phi \rightarrow qq)$ is a decay width of ϕ , and N_ϕ is the dimension of ϕ as a representation of $SU(3)_C$. The required $N_\phi \Gamma(\phi \rightarrow qq)$ are summarized in Table 3. Also, R_{LHC} and $R_{\text{Sp\bar{p}S}}$ is shown in Table 4 and 5, respectively. As is mentioned in Subsection 3.2, we require that the decay width of ϕ is lower than 15 GeV when applying the exclusion criteria based on the predicted production cross section of ϕ at Sp \bar{p} S. $R_{\text{Sp\bar{p}S}}$ does not depend on N_ϕ , but smaller N_ϕ can make the constraint loose because of large decay width. In Table 5, some particle can not be excluded for smaller $SU(3)_C$ representation, because the required decay width for the smaller representation is larger than 15 GeV.

All the operators are excluded from the ATLAS result unless the operators are composed of only valence quarks and ϕ . Even for operators composed of valence quarks, some

of them are excluded by the UA2 result.

4.1.2 Gluon- W boson - ϕ

The possible operators are

$$G_{\mu\nu}^a W^{\mu\nu} \phi^a \quad (4)$$

and its conjugate. These interaction terms give $W\phi$ signal by the diagrams shown in Fig. 1. The required coupling for 4 pb at the Tevatron can be translated into the decay width $\Gamma(\phi \rightarrow gW)$ of 8.5×10^{-2} GeV. This corresponds to the cutoff Λ of 850 GeV with the normalization $\frac{1}{\Lambda} G_{\mu\nu}^a W^{\mu\nu} \phi^a$. We estimate R_{LHC} is 8.6, then, this is excluded by the ATLAS result at 95 % C.L. [10]. As we mentioned at the beginning of this section, we do not analyze further with another operator which make ϕ decay into dijet.

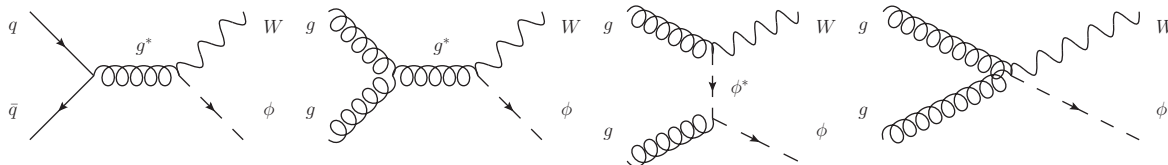


Figure 1: The diagrams contributing to the production of $W\phi$ by the operator $G_{\mu\nu}^a W^{\mu\nu} \phi^a$ at hadron colliders.

4.1.3 Photon or Z boson - W boson - ϕ

The possible operators are

$$B_{\mu\nu} W^{\mu\nu} \phi = (-\sin\theta_w Z_{\mu\nu} + \cos\theta_w F_{\mu\nu}) W^{\mu\nu} \phi \quad (5)$$

and its conjugate. These interaction terms give $W\phi$ signal by s-channel photon and Z boson exchange. The required decay width $\Gamma(\phi \rightarrow \gamma W)$ for 4 pb at the Tevatron is 7.3 GeV. This corresponds to the cutoff Λ of 100 GeV with the normalization $\frac{1}{\Lambda} B_{\mu\nu} W^{\mu\nu} \phi$. We estimate R_{LHC} is 3.4. Though this is not excluded by the ATLAS result, cut off of 100 GeV is not acceptable as a higher dimensional operator. Adding another operator to make ϕ decay into dijet and recalculating the required decay width inevitably lower this cut off, we do not further analyze. We can think of an operator like $W_{\mu\nu} W^{\mu\nu} \phi$. However, such operator will result in an unacceptably lower cutoff, too.

4.2 $X = V$: vector particle

Since there are a lot of possible operators to explain the WV production at the CDF, we pick up representative operators. Some variation of them are discussed in the text.

4.2.1 Quark - Quark - V : $V^\mu J_\mu$ type

The possible operators are

$$V^\mu q_L^\dagger \bar{\sigma}_\mu q_L \quad \text{or} \quad V^\mu q_L^\dagger \bar{\sigma}_\mu q_L^c \quad (6)$$

and their conjugates. These interaction terms give $W\phi$ signal by t-channel quark exchange diagrams. The following analysis is same as that of Subsection 4.1. The required $N_V \Gamma(V \rightarrow qq)$ are summarized in Table 6. R_{LHC} and R_{SppS} are shown in Table 7 and 8, respectively. As is mentioned in Subsubsection 4.1.1, the exclusion based of the UA2 result depend on which $SU(3)_C$ representation V obeys. All the operators which do not contain valence quarks are excluded by the ATLAS result.

4.2.2 Quark - quark- V : Pauli term type

The possible operators are

$$V_{\mu\nu} q_R^c \sigma^{\mu\nu} q_L \quad \text{or} \quad V_{\mu\nu} q_R^\dagger \sigma^{\mu\nu} q_L \quad (7)$$

and their conjugates where $\sigma^{\mu\nu} = \frac{i}{2}(\sigma^\mu \bar{\sigma}^\nu - \sigma^\nu \bar{\sigma}^\mu)$. These interaction terms give $W\phi$ signal by t-channel quark exchange diagrams. The following analysis is same as that of 4.1. The required $N_V \Gamma(V \rightarrow qq)$ are summarized in Table 9.

This can be also expressed in terms of the strength of the coupling. We have shown the required cut off Λ in Table 10 with the normalization

$$\frac{\sqrt{3}}{\sqrt{N_V} \Lambda} C_{ij}^r V_{\mu\nu}^r q_i^\dagger \sigma^{\mu\nu} q_j, \quad (8)$$

where q is two component quark field, i, j are the indexes of the color of quarks, r is the index of color of V , C_{ij}^r is the Clebsch-Gordan coefficients of the expansion $3(\bar{3}) \otimes 3(\bar{3})$ to the representation of $SU(3)_c$ which V obeys. Here, the Clebsch-Gordan coefficients are normalized to satisfy $\sum_{i,j} C_{ij}^r C_{ij}^{r'*} = \delta^{rr'}$ and $\sum_r C_{ij}^r C_{i'j'}^{r'*} = \delta_{ii'} \delta_{jj'}$. R_{LHC} and R_{SppS}

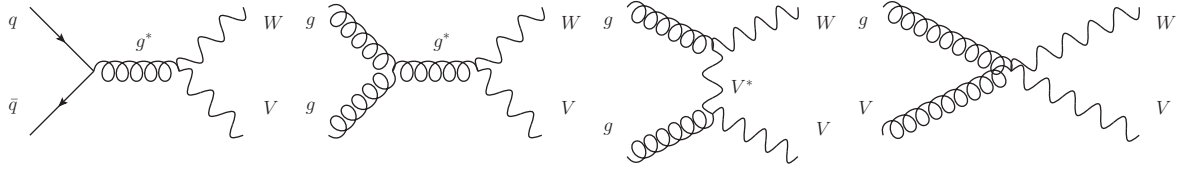


Figure 2: The diagrams contributing to the production of WV by the operator $G_{\mu\nu}^a W^\mu V^{a\nu}$ at hadron colliders.

are shown in Table 11 and 12, respectively. As is mentioned in Subsubsection 4.1.1, the exclusion based of the UA2 result depend on which $SU(3)_c$ representation V obeys. All the operators which do not contain valence quarks are excluded by the ATLAS result.

4.2.3 Gluon - W boson - V

The possible operators are

$$G_{\mu\nu}^a W^\mu V^{a\nu} \quad (9)$$

and its conjugate. These interaction terms give $W\phi$ signal by the diagrams shown in Fig. 2. The required decay width $\Gamma(V \rightarrow gW)$ is 3.4×10^{-2} GeV. We estimate R_{LHC} is 1.4×10^1 , then, this is excluded by the ATLAS result at 95 % C.L. [10]. As we mentioned at the beginning of this section, we do not analyze further with another operator which make ϕ decay into dijet since.

4.2.4 Photon or Z boson - W boson - V

The possible operators are

$$W_{\mu\nu}^3 W^\mu V^\nu = (\cos\theta_w Z_{\mu\nu} + \sin\theta_w F_{\mu\nu}) W^\mu V^\nu \quad (10)$$

and its conjugate. These interaction terms give WV signal by s-channel photon and Z boson exchange. The required decay width $\Gamma(V \rightarrow \gamma W)$ is 1.1 GeV. R_{LHC} is 6.8. This value is allowed by the ATLAS result at 95 % C.L. [10].

As we mentioned at the beginning of this section, we must add another operator to make V decay into dijet. This can be safely introduced without contradiction to Sp \bar{p} S nor LHC experiment. For example, take the decay width to $c\bar{s}$ to be 2 GeV and to γW to be

2 GeV so that production cross section of V and W boson times the branching fraction of V to dijet is 4 pb at the Tevatron. In this case, We estimate R_{SppS} is 0.1, which is not excluded. We estimate R_{LHC} is 7, which is also not excluded.

We can think of operators like $W_{\mu\nu}W_\mu^3V_\nu$, $B_{\mu\nu}W^\mu V^\nu$. These operators result in the similar cross section ratio. Therefore, such operators are still allowed, too.

4.3 $X = \psi$: spinor particle

4.3.1 Gluon - quark - ψ

The possible operators are

$$G_{\mu\nu}q_R^{c\dagger}\sigma^{\mu\nu}\psi_L \quad (11)$$

and their conjugates. These interaction terms give $W\phi$ signal by t-channel quark exchange diagrams. The following analysis is same as that of Subsection 4.1. The required $N_\psi\Gamma(\psi \rightarrow qg)$ are summarized in Table 13. The corresponding cut off Λ is shown in Table 14 in GeV with the normalization

$$\frac{2}{\sqrt{N_\psi}\Lambda}C_{ai}^rG_{\mu\nu}^aq_i^\dagger\sigma^{\mu\nu}\psi_L^r, \quad (12)$$

where q is the two component quark field, i is the index of the color of quark, r is the index of the color of ψ and C_{ai}^r is the Clebsch-Gordan coefficients of the expansion $8 \otimes 3(\bar{3})$ to the representation of $SU(3)_c$ which ψ obeys. Here, the Clebsch-Gordan coefficients are normalized to satisfy $\sum_{a,i}C_{ai}^rC_{ai}^{r'*} = \delta^{rr'}$ and $\sum_rC_{ai}^rC_{a'i'}^{r*} = \delta_{aa'}\delta_{ii'}$. R_{LHC} and R_{SppS} are shown in Table 15 and 16, respectively. All the operators are excluded by the ATLAS result at 95 % C.L. [10]. As is mentioned in Subsubsection 4.1.1, the exclusion based of the UA2 result depend on which $SU(3)_c$ representation V obeys.

We can think of operators like $W^\mu q^\dagger\sigma_\mu\psi$. However, since gluon is necessary for initial state in order to produce $W\psi$, such operator will result in exclusion by the ATLAS result, too.

5 Resonant production

In this section, we consider the case in which WX are produced by the decay of another particle Y , such as:

$$p + \bar{p}(p) \rightarrow Y \rightarrow W + X. \quad (13)$$

In calculating the production cross section, we use the narrow width approximation.³ Then, the production cross section is proportional to the decay width of $Y \rightarrow ij$. Here, i and j are initial partons. The production cross section is given by,

$$\sigma(Y) = C(i, j) \times N_Y \Gamma(Y \rightarrow ij), \quad (14)$$

where N_Y is the degree of freedom of the particle Y . The coefficient $C(i, j)$ is determined by the parton distribution function of incoming hadrons and do not depend on the detailed property of Y such as the spin and quantum numbers. Therefore, for each combination of i and j , we can calculate the required decay width for 4 pb at the Tevatron. The required $N_Y \Gamma(Y \rightarrow ij)$ are summarized in Table 17.

R_{LHC} , which depend only on the initial partons, is shown in Table 18. The operators including only valence quark are not excluded by the ATLAS result.

³ For some combinations of assumed initial partons, the required decay width for 4 pb at the Tevatron might go beyond the validity of the narrow width approximation. In such a case, as is shown later, the ratio of the production cross section of Y at the LHC with R_{LHC} is greater than 40. Since such operators are excluded by ATLAS result, we do not have to consider such operators from the beginning.

Table 3: $(\phi q_L^i q^j, 4.1.1)$ The required $N_\phi \Gamma(\phi \rightarrow qq) / 1 \text{ GeV}$ for the $W\phi$ cross section to be 4 pb at the Tevatron.

$i \backslash j$	\bar{b}	\bar{c}	\bar{s}	\bar{u}	\bar{d}
b	5.3×10^5	9.7×10^2	9.1×10^2	1.9×10^2	8.3×10^1
\bar{c}	9.7×10^2	2.8×10^2	2.3×10^2	2.1×10^1	2.7×10^1
\bar{s}	9.1×10^2	2.3×10^2	1.6×10^2	2.6×10^1	2.2×10^1
\bar{u}	1.9×10^2	2.1×10^1	2.6×10^1	6.8	9.9
d	8.3×10^1	2.7×10^1	2.2×10^1	9.9	6.9
d	8.3×10^1	5.0×10^1	3.1×10^1	1.8	3.8
u	1.9×10^2	1.2×10^2	7.0×10^1	3.8	8.4
s	9.1×10^2	5.4×10^2	3.3×10^2	2.0×10^1	4.4×10^1
c	9.7×10^2	5.6×10^2	3.4×10^2	2.1×10^1	4.6×10^1
b	1.1×10^6	6.2×10^5	3.7×10^5	2.3×10^4	5.2×10^4

Table 4: $(\phi q_L^i q^j, 4.1.1)$ The enhancement factor R_{LHC} defined in Eq. (1). The elements marked \circ and written in blue letters are NOT excluded by the ATLAS result.

$i \backslash j$	\bar{b}	\bar{c}	\bar{s}	\bar{u}	\bar{d}
b	6.5×10^1	5.9×10^1	4.8×10^1	3.8×10^1	2.9×10^1
\bar{c}	5.9×10^1	5.3×10^1	4.5×10^1	2.4×10^1	2.7×10^1
\bar{s}	4.8×10^1	4.5×10^1	3.8×10^1	2.7×10^1	2.4×10^1
\bar{u}	3.8×10^1	2.4×10^1	2.7×10^1	3.0×10^1	2.4×10^1
d	2.9×10^1	2.7×10^1	2.4×10^1	2.4×10^1	3.0×10^1
d	2.9×10^1	2.6×10^1	2.1×10^1	$\circ 2.9$	$\circ 5.0$
u	3.8×10^1	3.4×10^1	2.8×10^1	$\circ 5.1$	$\circ 8.0$
s	4.8×10^1	4.3×10^1	3.8×10^1	1.2×10^1	1.6×10^1
c	5.9×10^1	5.3×10^1	4.7×10^1	1.6×10^1	2.2×10^1
b	6.5×10^1	5.9×10^1	5.3×10^1	2.1×10^1	2.7×10^1

Table 5: $(\phi q_L^i q^j, 4.1.1)$ The enhancement factor R_{SppS} defined in Eq. (2). The elements marked \bullet and written in red letters are excluded by the UA2 result at 90 % C.L. [13] for ϕ which obeys any representation of $SU(3)_C$. * and green letters are excluded only $SU(3)_C$ higher representation, i.e., 8 or $6(\bar{6})$.

$i \backslash j$	\bar{b}	\bar{c}	\bar{s}	\bar{u}	\bar{d}
b	7.4×10^3	1.3×10^1	2.0×10^1	1.1×10^2	1.8×10^1
\bar{c}	1.3×10^1	1.5×10^1	10	2.3×10^1	1.1×10^1
\bar{s}	2.0×10^1	10	2.4×10^1	* 4.9×10^1	1.6×10^1
\bar{u}	1.1×10^2	2.3×10^1	* 4.9×10^1	$\bullet 7.3 \times 10^1$	$\bullet 4.3 \times 10^1$
d	1.8×10^1	1.1×10^1	1.6×10^1	$\bullet 4.3 \times 10^1$	3.2×10^1
d	1.8×10^1	2.1×10^1	2.2×10^1	$\bullet 4.2 \times 10^1$	3.6×10^1
u	1.2×10^2	1.3×10^2	1.3×10^2	$\bullet 2.1 \times 10^2$	* 2.0×10^2
s	2.0×10^1	2.3×10^1	2.4×10^1	3.8×10^1	3.1×10^1
c	1.3×10^1	1.5×10^1	1.5×10^1	2.2×10^1	1.9×10^1
b	7.4×10^3	8.4×10^3	8.4×10^3	1.4×10^4	1.1×10^4

Table 6: $(V_\mu q_L^i \sigma^\mu q^j, 4.2.1)$ The required $N_V \Gamma(V \rightarrow qq) / 1 \text{ GeV}$ for 4 pb at the Tevatron.

$i \backslash j$	\bar{b}	\bar{c}	\bar{s}	\bar{u}	\bar{d}
b	2.5×10^5	4.5×10^2	4.2×10^2	8.9×10^1	3.8×10^1
\bar{c}	4.5×10^2	1.3×10^2	9.1×10^1	9.7	1.2×10^1
\bar{s}	4.2×10^2	9.1×10^1	7.6×10^1	1.1×10^1	1.0×10^1
\bar{u}	8.9×10^1	9.7	1.1×10^1	3.1	3.5
d	3.8×10^1	1.2×10^1	1.0×10^1	3.5	3.2
d	3.8×10^1	2.3×10^1	1.4×10^1	7.6×10^{-1}	1.7
u	9.0×10^1	5.3×10^1	3.2×10^1	1.7	3.7
s	4.2×10^2	2.5×10^2	1.5×10^2	8.6	1.9×10^1
c	4.5×10^2	2.6×10^2	1.6×10^2	9.2	2.1×10^1
b	5.0×10^5	2.9×10^5	1.7×10^5	1.0×10^4	2.4×10^4

Table 7: ($V_\mu q_L^i \sigma^\mu q^j$, 4.2.1) The enhancement factor R_{LHC} for $V_\mu q_L^i \sigma^\mu q^j$.

$i \backslash j$	\bar{b}	\bar{c}	\bar{s}	\bar{u}	\bar{d}
b	9.1×10^1	8.3×10^1	6.7×10^1	5.3×10^1	4.2×10^1
\bar{c}	8.3×10^1	7.5×10^1	5.4×10^1	3.6×10^1	3.8×10^1
\bar{s}	6.7×10^1	5.4×10^1	5.4×10^1	3.8×10^1	3.6×10^1
\bar{u}	5.3×10^1	3.6×10^1	3.8×10^1	5.3×10^1	3.0×10^1
d	4.2×10^1	3.8×10^1	3.6×10^1	3.0×10^1	5.4×10^1
d	4.2×10^1	3.7×10^1	3.1×10^1	$\circ 4.0$	$\circ 7.1$
u	5.4×10^1	4.8×10^1	4.1×10^1	$\circ 7.2$	1.1×10^1
s	6.7×10^1	6.1×10^1	5.4×10^1	1.7×10^1	2.3×10^1
c	8.3×10^1	7.5×10^1	6.6×10^1	2.4×10^1	3.1×10^1
b	9.1×10^1	8.3×10^1	7.5×10^1	3.0×10^1	3.9×10^1

Table 8: ($V_\mu q_L^i \sigma^\mu q^j$, 4.2.1) The enhancement factor R_{SppS} for $V_\mu q_L^i \sigma^\mu q^j$.

$i \backslash j$	\bar{b}	\bar{c}	\bar{s}	\bar{u}	\bar{d}
b	5.2×10^3	5.4×10^3	5.9×10^3	1.1×10^4	9.4×10^3
\bar{c}	9.2	1.0×10^1	9.6	1.9×10^1	1.6×10^1
\bar{s}	1.4×10^1	1.6×10^1	1.6×10^1	$* 5.1 \times 10^1$	3.8×10^1
\bar{u}	8.0×10^1	8.7×10^1	$* 9.2 \times 10^1$	$\bullet 5.0 \times 10^1$	$\bullet 6.6 \times 10^1$
d	1.3×10^1	1.4×10^1	1.5×10^1	3.5×10^1	2.2×10^1
d	1.3×10^1	6.8	8.7	2.2×10^1	1.2×10^1
u	7.9×10^1	1.3×10^1	1.9×10^1	$\bullet 6.8 \times 10^1$	2.2×10^1
s	1.4×10^1	6.3	8.2	1.9×10^1	8.7
c	9.2	5.1	6.3	1.3×10^1	6.8
b	2.6×10^3	9.2	1.4×10^1	7.9×10^1	1.3×10^1

Table 9: ($V_{\mu\nu}q_L^i\sigma^{\mu\nu}q^j$, 4.2.2) The required $N_V\Gamma(V \rightarrow qq) / 1 \text{ GeV}$ for 4 pb at the Tevatron.

$i \backslash j$	\bar{b}	\bar{c}	\bar{s}	\bar{u}	\bar{d}
b	6.8×10^4	1.2×10^2	1.1×10^2	2.4×10^1	1.0×10^1
\bar{c}	1.2×10^2	3.6×10^1	3.2×10^1	2.6	3.3
\bar{s}	1.1×10^2	3.2×10^1	2.0×10^1	3.2	2.7
\bar{u}	2.4×10^1	2.6	3.2	8.2×10^{-1}	1.4
d	1.0×10^1	3.3	2.7	1.4	8.3×10^{-1}
d	1.0×10^1	6.0	3.7	1.8×10^{-1}	4.2×10^{-1}
u	2.4×10^1	1.4×10^1	8.7	4.1×10^{-1}	9.5×10^{-1}
s	1.1×10^2	6.7×10^1	4.1×10^1	2.2	5.0
c	1.2×10^2	7.2×10^1	4.3×10^1	2.4	5.6
b	1.4×10^5	7.8×10^4	4.8×10^4	2.7×10^3	6.3×10^3

Table 10: ($V_{\mu\nu}q_L^i\sigma^{\mu\nu}q^j$, 4.2.2) The required cut off Λ in GeV for 4 pb at the Tevatron. See the text for the definition of Λ .

$i \backslash j$	\bar{b}	\bar{c}	\bar{s}	\bar{u}	\bar{d}
b	1.4	4.7×10^1	4.9×10^1	1.1×10^2	1.6×10^2
\bar{c}	4.7×10^1	6.1×10^1	9.2×10^1	3.2×10^2	2.8×10^2
\bar{s}	4.9×10^1	9.2×10^1	8.1×10^1	2.9×10^2	3.2×10^2
\bar{u}	1.1×10^2	3.2×10^2	2.9×10^2	4.0×10^2	4.4×10^2
d	1.6×10^2	2.8×10^2	3.2×10^2	4.4×10^2	4.0×10^2
d	1.6×10^2	2.1×10^2	2.7×10^2	1.2×10^3	8.0×10^2
u	1.1×10^2	1.4×10^2	1.8×10^2	8.1×10^2	5.3×10^2
s	4.9×10^1	6.4×10^1	8.1×10^1	3.5×10^2	2.3×10^2
c	4.7×10^1	6.1×10^1	7.9×10^1	3.4×10^2	2.2×10^2
b	1.4	1.9	2.4	10	6.5

Table 11: $(V_{\mu\nu}q_L^i\sigma^{\mu\nu}q^j, 4.2.2)$ The enhancement factor R_{LHC} for $V_{\mu\nu}q_L^i\sigma^{\mu\nu}q^j$.

$i \backslash j$	\bar{b}	\bar{c}	\bar{s}	\bar{u}	\bar{d}
b	9.5×10^1	8.8×10^1	7.2×10^1	6.0×10^1	4.8×10^1
\bar{c}	8.8×10^1	8.0×10^1	5.1×10^1	4.3×10^1	4.4×10^1
\bar{s}	7.2×10^1	5.1×10^1	5.9×10^1	4.4×10^1	4.4×10^1
\bar{u}	6.0×10^1	4.3×10^1	4.4×10^1	7.5×10^1	3.8×10^1
d	4.8×10^1	4.4×10^1	4.4×10^1	3.8×10^1	7.6×10^1
\bar{d}	4.8×10^1	4.3×10^1	3.7×10^1	$\circ 4.5$	$\circ 8.2$
u	6.0×10^1	5.4×10^1	4.7×10^1	$\circ 8.3$	1.3×10^1
s	7.2×10^1	6.5×10^1	5.9×10^1	1.9×10^1	2.5×10^1
c	8.8×10^1	8.0×10^1	7.2×10^1	2.8×10^1	3.6×10^1
b	9.5×10^1	8.6×10^1	7.9×10^1	3.4×10^1	4.3×10^1

Table 12: $(V_{\mu\nu}q_L^i\sigma^{\mu\nu}q^j, 4.2.2)$ The enhancement factor R_{SppS} for $V_{\mu\nu}q_L^i\sigma^{\mu\nu}q^j$. Same as Table 5.

$i \backslash j$	\bar{b}	\bar{c}	\bar{s}	\bar{u}	\bar{d}
b	2.8×10^3	5.1	7.6	$* 4.3 \times 10^1$	6.7
\bar{c}	5.1	5.6	4.2	8.4	4.1
\bar{s}	7.6	4.2	8.8	1.8×10^1	5.7
\bar{u}	$* 4.3 \times 10^1$	8.4	1.8×10^1	2.6×10^1	1.8×10^1
d	6.7	4.1	5.7	1.8×10^1	1.2×10^1
\bar{d}	6.7	7.5	7.9	1.3×10^1	1.2×10^1
u	$* 4.3 \times 10^1$	$* 4.7 \times 10^1$	$* 5.0 \times 10^1$	$\bullet 6.8 \times 10^1$	$\bullet 6.7 \times 10^1$
s	7.6	8.7	8.8	1.2×10^1	1.1×10^1
c	5.1	5.6	5.7	7.8	6.9
b	2.8×10^3	3.2×10^3	3.2×10^3	4.8×10^3	4.1×10^3

Table 13: ($G_{\mu\nu}q^\dagger\sigma^{\mu\nu}\psi$, 4.3.1) The required $N_\psi\Gamma(\psi \rightarrow qg) / 1 \text{ GeV}$ for 4 pb at the Tevatron.

	b	\bar{c}	\bar{s}	\bar{u}	d
g	3.1×10^1	1.8×10^1	1.1×10^1	6.7×10^{-1}	1.6

Table 14: ($G_{\mu\nu}q^\dagger\sigma^{\mu\nu}\psi$, 4.3.1) The required cut off Λ . See the text for the definition of Λ .

	b	\bar{c}	\bar{s}	\bar{u}	d
g	1.9×10^2	2.4×10^2	3.1×10^2	1.3×10^3	8.3×10^2

Table 15: ($G_{\mu\nu}q^\dagger\sigma^{\mu\nu}\psi$, 4.3.1) The enhancement factor R_{LHC} for $G_{\mu\nu}q^\dagger\sigma^{\mu\nu}\psi$.

	b	\bar{c}	\bar{s}	\bar{u}	d
g	9.5×10^1	8.7×10^1	7.9×10^1	3.8×10^1	4.8×10^1

Table 16: ($G_{\mu\nu}q^\dagger\sigma^{\mu\nu}\psi$, 4.3.1) The enhancement factor R_{SppS} for $G_{\mu\nu}q^\dagger\sigma^{\mu\nu}\psi$.

	b	\bar{c}	\bar{s}	\bar{u}	d
g	* 2.1×10^2	• 2.4×10^2	• 2.4×10^2	• 3.5×10^2	• 3.2×10^2

Table 17: (Resonance, 5) The required $N_Y \Gamma(Y \rightarrow ij) / 1 \text{ GeV}$ for the Y cross section to be 4 pb at the Tevatron.

$i \backslash j$	\bar{b}	\bar{c}	\bar{s}	\bar{u}	\bar{d}	g
b	6.6×10^1	3.8×10^1	2.3×10^1	1.5	3.5	4.2
\bar{c}	3.8×10^1	2.2×10^1	1.3×10^1	9.4×10^{-1}	2.1	2.4
\bar{s}	2.3×10^1	1.3×10^1	8	5.8×10^{-1}	1.3	1.5
\bar{u}	1.5	9.4×10^{-1}	5.8×10^{-1}	2.2×10^{-1}	2.6×10^{-1}	1.1×10^{-1}
d	3.5	2.1	1.3	2.6×10^{-1}	4.1×10^{-1}	2.3×10^{-1}
g	4.2	2.4	1.5	1.1×10^{-1}	2.3×10^{-1}	2.7×10^{-1}
d	3.5	2.1	1.3	9.3×10^{-2}	1.8×10^{-1}	2.3×10^{-1}
u	1.5	9.4×10^{-1}	5.8×10^{-1}	4.9×10^{-2}	9.3×10^{-2}	1.1×10^{-1}
s	2.3×10^1	1.3×10^1	8	5.8×10^{-1}	1.3	1.5
c	3.8×10^1	2.2×10^1	1.3×10^1	9.4×10^{-1}	2.1	2.4
b	6.6×10^1	3.8×10^1	2.3×10^1	1.5	3.5	4.2

Table 18: (Resonance, 5) The enhancement factor R_{LHC} . The elements marked \circ and written in blue letters are NOT excluded by the ATLAS result.

	b	\bar{c}	\bar{s}	\bar{u}	\bar{d}	g
b	7.4×10^1	6.7×10^1	5.8×10^1	2.2×10^1	2.9×10^1	6.1×10^1
\bar{c}	6.7×10^1	6.1×10^1	5.2×10^1	1.9×10^1	2.6×10^1	5.5×10^1
\bar{s}	5.8×10^1	5.2×10^1	4.4×10^1	1.5×10^1	2.1×10^1	4.7×10^1
\bar{u}	2.2×10^1	1.9×10^1	1.5×10^1	1.7×10^1	1.5×10^1	1.8×10^1
d	2.9×10^1	2.6×10^1	2.1×10^1	1.5×10^1	1.6×10^1	2.4×10^1
g	6.1×10^1	5.5×10^1	4.7×10^1	1.8×10^1	2.4×10^1	5.0×10^1
d	2.9×10^1	2.6×10^1	2.1×10^1	$\circ 4.1$	$\circ 6.2$	2.4×10^1
u	2.2×10^1	1.9×10^1	1.5×10^1	$\circ 2.6$	$\circ 4.1$	1.8×10^1
s	5.8×10^1	5.2×10^1	4.4×10^1	1.5×10^1	2.1×10^1	4.7×10^1
c	6.7×10^1	6.1×10^1	5.2×10^1	1.9×10^1	2.6×10^1	5.5×10^1
b	7.4×10^1	6.7×10^1	5.8×10^1	2.2×10^1	2.9×10^1	6.1×10^1

6 Possible improvement of the search at LHC

In the previous sections, we find that some operators are insensitive to the current search at the LHC 7 TeV run and the Sp \bar{p} S. We list such cases here;

$$\phi d_R^\dagger d_L, \phi d_R^\dagger u_L, V^\mu u_L^\dagger \bar{\sigma}_\mu d_L, V^\mu u_L^\dagger \bar{\sigma}_\mu d_L, V^{\mu\nu} u_R^\dagger \bar{\sigma}_{\mu\nu} d_L, V^{\mu\nu} d_R^\dagger \bar{\sigma}_{\mu\nu} d_L$$

Resonant production, the initial partons are $d\bar{u}$, $u\bar{u}$, $d\bar{d}$ (15)

In this section, we study a possible improvement of the search at the LHC 7 TeV run. We apply the following selection cuts in addition to the ones used in Ref. [10].

1. The leading two jets have p_T larger than 100 and 50 GeV,
2. There is only one lepton which is required to have p_T larger than 90 GeV,
3. \cancel{E}_T is larger than 90 GeV,
4. $140 \text{ GeV} < M_{jj} < 160 \text{ GeV}$.

Here p_T , \cancel{E}_T and M_{jj} are the transverse momentum, the transverse missing energy and the invariant mass of the leading two jets, respectively. The number of the remaining background events after applying all the cuts are summarized in Table. 19. We also summarize the acceptance of the signal for some representative cases in Table. 20. Unfortunately, the acceptances of the signals strongly depend on the operators which produce the Wjj signal with the severe cut we apply. Especially, in the cases of the resonant production, the acceptances are too small that the signals are not observed in the LHC. Such low acceptances is expected because the energies of W and X are restricted by the mass of the parent particle Y . We must use more sophisticated techniques to search for the resonant production, which is model-dependent and beyond the scope of this article. In the case of the operator $V_{\mu\nu} u_R^\dagger \sigma^{\mu\nu} d_L$, the acceptance is rather high. This is because the operator is the higher dimensional one and the cross section do not drop down at high energy. To estimate the expected constraints on the operators, it is conservative to use the acceptance for the operator $\phi u_L^\dagger d_R$, which is renormalizable. For the non-resonant production, with the use of the conservative acceptance, the expected 95% C.L. constraints on R_{LHC} is $R_{\text{LHC}} < 1.4$ with 5 fb^{-1} data. Here we assign the same degree of systematic error as the one in Ref. [10]. This expected constraint covers all the operators we list in

Table 19: The expected number of the events after applying all the selection cuts listed in Sec. 6 in addition to the ones applied in Ref. [10] at the LHV 7 TeV run.

	Number of the events /fb ⁻¹
$W + \text{jets}$	50.3
$t\bar{t} + \text{jets}$	52.5

Table 20: The acceptance of the signal after applying all the selection cuts listed in Sec. 6 in addition to the ones applied in Ref. [10] at the LHV 7 TeV run.

	Acceptances
$\phi u_L^\dagger d_R$	0.013
$V_{\mu\nu} u_R^\dagger \sigma^{\mu\nu} d_L$	0.035
Resonant production, initial parton are $\bar{d}u$	0

Sec. 4. Since we use the fast simulation, this expected constraint is just a rough estimate. Especially, the systematic error should be evaluated based on the actual experiments.

7 Conclusion and Discussion

In this paper, we discuss testability of the CDF Wjj anomaly at the LHC. We comprehensively study models which can realize Wjj signal observed by the CDF collaboration. We have found that the cross section at the LHC mainly depends on what partons in p and \bar{p} produce W and X and that almost all the models are inconsistent with the result of the LHC, unless only valence quarks contribute the new process. We list the allowed cases in Eq. (15). We also study the possible improvement of the search at LHC. We have found that by using the more severe cuts than the one used in [10], it might be possible to discover/exclude the Wjj signal for any models except for the case of resonant production. As mentioned in footnote 1, some models are not within our study. However, even in such a case, the cross section at the LHC is expected to be $\mathcal{O}(1) \times \sigma_{\text{Tevatron}}$ in the case of production by valence quarks and $\mathcal{O}(10 - 100) \times \sigma_{\text{Tevatron}}$ for sea quarks or gluons case. In the latter case, the ATLAS result gives strong constraint.

Acknowledgement

This work was supported by the World Premier International Research Center Initiative (WPI Initiative), MEXT, Japan. The work of RS and SS is supported in part by JSPS Research Fellowships for Young Scientists.

References

- [1] T. Aaltonen *et al.* [CDF Collaboration], Phys. Rev. Lett. **106** (2011) 171801 [arXiv:1104.0699 [hep-ex]].
- [2] M. R. Buckley, D. Hooper, J. Kopp, E. Neil, [arXiv:1103.6035 [hep-ph]]; F. Yu, Phys. Rev. **D83**, 094028 (2011). [arXiv:1104.0243 [hep-ph]]; X. -P. Wang, Y. -K. Wang, B. Xiao, J. Xu, S. -h. Zhu, [arXiv:1104.1161 [hep-ph]]; K. Cheung, J. Song, [arXiv:1104.1375 [hep-ph]]; X. -P. Wang, Y. -K. Wang, B. Xiao, J. Xu, S. -h. Zhu, [arXiv:1104.1917 [hep-ph]]; L. A. Anchordoqui, H. Goldberg, X. Huang, D. Lust, T. R. Taylor, [arXiv:1104.2302 [hep-ph]]; S. Jung, A. Pierce, J. D. Wells, [arXiv:1104.3139 [hep-ph]]; P. Ko, Y. Omura, C. Yu, [arXiv:1104.4066 [hep-ph]];

- P. J. Fox, J. Liu, D. Tucker-Smith, N. Weiner, [arXiv:1104.4127 [hep-ph]]; D. - W. Jung, P. Ko, J. S. Lee, [arXiv:1104.4443 [hep-ph]]; S. Chang, K. Y. Lee, J. Song, [arXiv:1104.4560 [hep-ph]]; X. Huang, [arXiv:1104.5389 [hep-ph]]; Z. Liu, P. Nath, G. Peim, [arXiv:1105.4371 [hep-ph]]; J. L. Hewett, T. G. Rizzo, [arXiv:1106.0294 [hep-ph]]; A. E. Faraggi, V. M. Mehta, [arXiv:1106.5422 [hep-ph]]; L. Vecchi, [arXiv:1107.2933 [hep-ph]].
- [3] C. Kilic, S. Thomas, [arXiv:1104.1002 [hep-ph]]; A. E. Nelson, T. Okui, T. S. Roy, [arXiv:1104.2030 [hep-ph]]; B. A. Dobrescu, G. Z. Krnjaic, [arXiv:1104.2893 [hep-ph]]; Q. -H. Cao, M. Carena, S. Gori, A. Menon, P. Schwaller, C. E. M. Wagner, L. -T. Wang, [arXiv:1104.4776 [hep-ph]]; B. Dutta, S. Khalil, Y. Mimura, Q. Shafi, [arXiv:1104.5209 [hep-ph]]; L. M. Carpenter, S. Mantry, [arXiv:1104.5528 [hep-ph]]; G. Segre, B. Kayser, [arXiv:1105.1808 [hep-ph]]; T. Enkhbat, X. -G. He, Y. Mimura, H. Yokoya, [arXiv:1105.2699 [hep-ph]]; C. -H. Chen, C. -W. Chiang, T. Nomura, Y. Fusheng, [arXiv:1105.2870 [hep-ph]]; A. Alves, E. R. Barreto, A. G. Dias, [arXiv:1105.4849 [hep-ph]]; J. Fan, D. Krohn, P. Langacker, I. Yavin, [arXiv:1106.1682 [hep-ph]]; J. Evans, B. Feldstein, W. Klemm, H. Murayama, T. T. Yanagida, [arXiv:1106.1734 [hep-ph]]; J. F. Gunion, [arXiv:1106.3308 [hep-ph]]; D. K. Ghosh, M. Maity, S. Roy, [arXiv:1107.0649 [hep-ph]].
- [4] G. Isidori, J. F. Kamenik, Phys. Lett. **B700**, 145-149 (2011). [arXiv:1103.0016 [hep-ph]]; R. Sato, S. Shirai, K. Yonekura, Phys. Lett. **B700**, 122-125 (2011). [arXiv:1104.2014 [hep-ph]].
- [5] L. A. Anchordoqui, W. -Z. Feng, H. Goldberg, X. Huang, T. R. Taylor, Phys. Rev. **D83**, 106006 (2011). [arXiv:1012.3466 [hep-ph]]; E. J. Eichten, K. Lane, A. Martin, [arXiv:1104.0976 [hep-ph]]; H. B. Nielsen, [arXiv:1104.4642 [hep-ph]]; K. S. Babu, M. Frank, S. K. Rai, [arXiv:1104.4782 [hep-ph]]; R. Harnik, G. D. Kribs, A. Martin, [arXiv:1106.2569 [hep-ph]]; Y. Cui, Z. Han, M. D. Schwartz, [arXiv:1106.3086 [hep-ph]]. R. Fok, G. D. Kribs, [arXiv:1106.3101 [hep-ph]].
- [6] X. -G. He and B. -Q. Ma, Eur. Phys. J. A **47**, 152 (2011) [arXiv:1104.1894 [hep-ph]]; Z. Sullivan and A. Menon, Phys. Rev. D **83**, 091504 (2011) [arXiv:1104.3790 [hep-ph]].

- ph]]; T. Plehn and M. Takeuchi, J. Phys. G **38**, 095006 (2011) [arXiv:1104.4087 [hep-ph]].
- [7] V. M. Abazov *et al.* [D0 Collaboration], arXiv:1106.1921 [hep-ex].
- [8] E. Eichten, K. Lane, A. Martin, [arXiv:1107.4075 [hep-ph]].
- [9] A. Annovi, P. Catastini, V. Cavaliere, L. Ristori, “Kinematic Distribution of events in the $115 < M_{JJ} < 175$ GeV region.”
<http://www-cdf.fnal.gov/physics/ewk/2011/wjj/kinematics.html>
- [10] The ATLAS Collaboration, “Invariant mass distribution of jet pairs produced in association with a leptonically decaying W boson using 1.02 fb^{-1} of ATLAS data”, ATLAS-CONF-2011-097,
<http://cdsweb.cern.ch/record/1369206/files/ATLAS-CONF-2011-097.pdf>
- [11] J. Alwall, P. Demin, S. de Visscher, R. Frederix, M. Herquet, F. Maltoni, T. Plehn, D. L. Rainwater *et al.*, JHEP **0709**, 028 (2007). [arXiv:0706.2334 [hep-ph]].
- [12] L. Moneta, K. Belasco, K. Cranmer, A. Lazzaro, D. Piparo, G. Schott, W. Verkerke, M. Wolf *et al.*, PoS **ACAT2010**, 057 (2010). [arXiv:1009.1003 [physics.data-an]].
- [13] J. Alitti *et al.* [UA2 Collaboration], Nucl. Phys. **B400**, 3-24 (1993).
- [14] D. Stump, J. Huston, J. Pumplin, W. -K. Tung, H. L. Lai, S. Kuhlmann, J. F. Owens, JHEP **0310**, 046 (2003). [hep-ph/0303013].